Research Square

Preprints are preliminary reports that have not undergone peer review.
They should not be considered conclusive, used to inform clinical practice,
or referenced by the media as validated information.

TRIM36 Catalyzes K63-Linked Ubiquitination of TAK1 to Drive Septic Inflammation

Shijie Song
Guangzhou Medical University
Dingnai Nie
Guangzhou Medical University
Zulaya Abudureyimu
Guangzhou Medical University
Yijin Kuang
Southern Medical University
Wen Li
Guangzhou Medical University
Xiaodan Yang
Guangzhou Medical University
Qiao Ling
Guangzhou Medical University
Junli Sheng
Guangzhou Medical University
Huiru He
Guangzhou Medical University
Xiaolong You
Guangzhou Medical University
Suwan Wu
Guangzhou Medical University
Wenhao Wu
Guangzhou Medical University
Yuling Fu
Guangzhou Medical University
Shouhai Wu
The Second Affiliated Hospital of Guangzhou University of Chinese Medicine
Kang Chen
Zhongshan City People's Hospital
Shengfeng Hu
hushengfeng@gzhmu.edu.cn

Guangzhou Medical University

Research Article

Keywords: Sepsis, TRIM36, TAK1, Macrophage, TLR4

Posted Date: June 28th, 2026

DOI: https://doi.org/10.21203/rs.3.rs-9884192/v1

License: This work is licensed under a Creative Commons Attribution 4.0 International License.
Read Full License

Additional Declarations: No competing interests reported.

Version of Record: A version of this preprint was published at Inflammation Research on October 17th, 2026. See the published version at https://doi.org/10.1007/s00011-026-02393-5.

Abstract

The Toll-like receptor 4 (TLR4) pathway is critical for initiating innate immunity; however, its dysregulation drives pathological inflammation in diseases such as sepsis. Here, we identify tripartite motif protein 36 (TRIM36) as a key positive regulator that amplifies TLR4 signaling. TRIM36 expression was robustly upregulated in macrophages upon lipopolysaccharide (LPS) challenge. Mechanistically, TRIM36 directly bound to TGF-β-activated kinase 1 (TAK1) and catalyzed its K63-linked ubiquitination, a prerequisite for the activation of TAK1 and the downstream nuclear factor-κB (NF-κB) pathway. Functionally, genetic ablation of Trim36 in mice attenuated hypothermia, improved survival, and reduced cytokine production in an LPS-induced sepsis model. Consistently, in vitro knockdown of TRIM36 in human macrophages blunted LPS-induced signaling and the secretion of proinflammatory mediators. Furthermore, analysis of a public transcriptomic dataset revealed that elevated TRIM36 levels were associated with non-survival in patients with sepsis. Collectively, our findings establish TRIM36 as a critical amplifier of TLR4-induced hyperinflammation and highlight its potential as a therapeutic target for sepsis.

Introduction

Sepsis is a life-threatening condition caused by a dysregulated host response to infection and remains a leading cause of death worldwide[1]. Despite extensive research efforts, no specific therapeutic interventions beyond intensive care unit (ICU) support are currently available for sepsis[2]. Patient prognosis is governed by the dynamic interplay between pro-inflammatory and anti-inflammatory responses within the host immune system[2]. The polarization status of macrophages exerts a deterministic influence on the immunological profile of septic patients. During distinct phases of sepsis, these innate immune cells undergo dynamic phenotypic reprogramming. Specifically, early hyperinflammatory stages are characterized by a microenvironment dominated by pro-inflammatory mediators (e.g., TNF-α and IL-6), which drive M1-like macrophage polarization and are associated with progressive expansion of the immunostimulatory macrophage population[3]. Upon recognition of pathogen-associated molecular patterns (PAMPs) or damage-associated molecular patterns (DAMPs), macrophage activation triggers pattern recognition receptor (PRR)-mediated production of proinflammatory mediators. This process initiates canonical inflammatory signaling cascades, predominantly through the nuclear factor-κB (NF-κB) and mitogen-activated protein kinase (MAPK) pathways, thereby inducing the release of key inflammatory cytokines, including interleukin-6 (IL-6), IL-1β, and tumor necrosis factor-alpha (TNF-α)[4, 5].

The NF-κB signaling pathway is a well-characterized molecular cascade that plays a pivotal role in modulating inflammatory and immune responses. In sepsis, TLR4 activation recruits the adaptor proteins MyD88 and TIR domain-containing adaptor protein (TIRAP), which sequentially activate IRAK1/4 kinases and promote TRAF6 ubiquitination, thereby mediating TLR-triggered NF-κB signal transduction through the IκB kinase (IKK) complex[6]. During this signaling cascade, transforming growth factor β-activated kinase 1 (TAK1) functions as a pivotal regulatory kinase that potentiates macrophage-

mediated inflammation. During this signaling cascade, transforming growth factor β-activated kinase 1 (TAK1) functions as a pivotal regulatory kinase that potentiates macrophage-mediated inflammation. This post-translational modification cascade ultimately leads to nuclear translocation of NF-κB, enabling transcriptional activation of pro-inflammatory genes[7]. Inhibition of TAK1 has been shown to be effective in ameliorating sepsis[8].

Ubiquitination is a post-translational modification that participates in diverse cellular processes, including the regulation of TLR4 signaling[9]. Ubiquitin is a highly conserved 76-amino acid protein that contains seven lysine residues (K6, K11, K27, K29, K33, K48, and K63). Ubiquitin chains undergo elongation via these residues[10]. Ubiquitination is enzymatically regulated by a tripartite system consisting of ubiquitin-activating enzymes (E1), ubiquitin-conjugating enzymes (E2), and ubiquitin ligases (E3)[11]. E1 enzymes initiate the process through ATP-dependent activation, E2 enzymes are responsible for substrate recognition and transfer, and E3 ligases catalyze the final isopeptide bond formation[11]. E3 ligases determine substrate specificity by engaging target proteins through specialized structural domains, thereby orchestrating precise ubiquitin transfer during the enzymatic cascade[12]. Different combinations of ubiquitin chains form various structures, each involved in specific biological functions such as proteasomal degradation or immune signaling[13–15]. The most prevalent polyubiquitin chain types are K48-linked and K63-linked modifications, which primarily mediate proteasomal degradation and intracellular signaling, respectively[16, 17]. Tripartite motif (TRIM) proteins represent a major subclass of E3 ubiquitin ligases and are characterized by conserved RING, B-box, and coiled-coil domains. This evolutionarily conserved family comprises over 70 distinct members in humans and plays pivotal roles in innate immunity and antiviral defense through substrate-specific ubiquitination[18]. Members of the TRIM family have been shown to participate in the regulation of TLR signaling pathways[19–24]. However, the role of the TRIM family in sepsis remains largely unexplored.

TRIM36 is a 728-amino acid protein in humans. It was initially identified in mice in 2003 as Haprin through characterization of a haploid germ cell-specific cDNA library derived from murine testes[25]. In humans, TRIM36 deficiency has been genetically associated with microtubule-related abnormalities and neural tube closure defects, including craniorachischisis and disrupted mitotic spindle formation[26]. Consequently, recent studies have predominantly focused on the role of TRIM36 in tumor growth regulation[27–29]. However, whether TRIM36 regulates the TLR signaling pathway remains unknown.

In this study, we identified TRIM36 as a critical positive regulator of septic inflammation and elucidated its underlying molecular mechanism. We found that LPS stimulation upregulated TRIM36 expression in macrophages and that TRIM36 deficiency attenuated systemic inflammatory responses and the hypersecretion of pro-inflammatory cytokines. Mechanistically, TRIM36 directly interacted with TAK1 and catalyzed its K63-linked ubiquitination at lysine 158, thereby facilitating the conformational changes required for TAK1 autophosphorylation and subsequent activation of NF-κB. Collectively, our findings establish TRIM36 as a novel amplifier of hyperinflammation in sepsis and highlight its potential as a therapeutic target for this life-threatening condition.

Results

TRIM36 mediates LPS-induced pro-inflammatory responses in macrophages

To investigate the potential involvement of TRIM family proteins in the immune response to LPS, we treated bone marrow-derived macrophages (BMDMs) with LPS and profiled the expression of TRIM family members by quantitative real-time PCR (qPCR). This screening revealed that, whereas most TRIM genes remained unchanged, TRIM36 expression was the most significantly induced (Fig. 1A). Analysis of public GEO datasets (GSE13904 and GSE28750) showed that TRIM36 transcript levels were substantially higher in patients with sepsis than in healthy controls (Fig. 1B, C). To validate these findings, we stimulated mouse BMDMs and the human monocytic cell line THP-1 with LPS and monitored TRIM36 expression by qPCR and western blotting. The results demonstrated a concordant upregulation of TRIM36 at both the mRNA and protein levels (Fig. 1D, E). To delineate the functional impact of TRIM36 on LPS-triggered responses, we isolated BMDMs from *Trim36*$^{+/+}$ and *Trim36*$^{-/-}$ mice and treated them with LPS for various durations. Compared with *Trim36*$^{+/+}$ BMDMs, *Trim36*$^{-/-}$ BMDMs exhibited a marked reduction in the production of pro-inflammatory mediators (IL-1β, IL-6, TNF-α, and NO), as measured by both gene transcription and protein secretion in the culture supernatant. Collectively, these results indicate that LPS stimulation enhances TRIM36 expression in macrophages and that TRIM36 plays a critical pro-inflammatory role in this setting.

TRIM36 deficiency protects mice from LPS-induced sepsis

To investigate the impact of TRIM36 on septic pathophysiology, we established an endotoxemia-based sepsis model by intraperitoneal (i.p.) administration of LPS (10 mg/kg) in *Trim36*$^{+/+}$ and *Trim36*$^{-/-}$ mice (Fig. 2A). Notably, compared with *Trim36*$^{+/+}$ littermates, *Trim36*$^{-/-}$ mice exhibited significantly improved survival rates and attenuated hypothermia progression following LPS challenge (Fig. 2B, C). Histopathological examination of lung tissue, a key injury site in sepsis, confirmed that TRIM36 deficiency alleviated sepsis-induced pulmonary injury (Fig. 2D). We next analyzed the levels of inflammatory cytokines in bronchoalveolar lavage fluid (BALF) and serum. Compared with the *Trim36*$^{+/+}$ group, the *Trim36*$^{-/-}$ group showed significantly reduced levels of IL-1β, IL-6, TNF-α, and NO (Fig. 2E, F). As macrophages are the primary inflammatory responders in sepsis, we performed flow cytometric analysis, which revealed a decreased proportion of F4/80^{+}CD11b^{+} peritoneal macrophages in *Trim36*$^{-/-}$ mice compared with *Trim36*$^{+/+}$ mice (Fig. S1A). Furthermore, the expression levels of CD80 and CD86, surface markers characteristic of inflammatory (M1) macrophages, were significantly lower in the *Trim36*$^{-/-}$ group (Fig. S1B). Collectively, these results demonstrate that TRIM36 acts as a critical driver of pro-inflammatory macrophage activation and exacerbates the pathogenesis of sepsis.

TRIM36 deficiency selectively impairs the TAK1-NF-κB axis downstream of TLR4

Macrophage activation in sepsis is frequently associated with activation of the TLR4 signaling pathway[30]. Canonical inflammatory pathways, including NF-κB, Janus kinase/signal transducer and activator of transcription (JAK/STAT), and mitogen-activated protein kinase (MAPK) cascades, play critical roles in mediating inflammatory activation during septic progression[6, 31, 32]. To further investigate the effects of TRIM36 on these pathways, we examined the phosphorylation status of key proteins in selected major signaling pathways after LPS stimulation. The results revealed that TRIM36 deficiency led to a notable decrease in p65 phosphorylation, whereas the phosphorylation levels of TBK1, IRF3, AKT, JNK, and p38 remained unaffected (Fig. 3A, B). To substantiate these findings, we assessed the phosphorylation of other critical signaling molecules downstream of TLR4. Following LPS stimulation at various time points, we found that TRIM36 deficiency markedly decreased the phosphorylation of TAK1 and IκBα, molecules known to promote downstream NF-κB signaling and inflammation (Fig. 3C, D). Finally, we performed RNA-seq on LPS-stimulated BMDMs from *Trim36*$^{+/+}$ and *Trim36*$^{-/-}$ mice. Gene Set Enrichment Analysis (GSEA) confirmed that, compared with *Trim36*$^{+/+}$ BMDMs, *Trim36*$^{-/-}$ BMDMs exhibited a negative enrichment signature for various inflammatory signaling pathways, including TOLL_LIKE_RECEPTOR_SIGNALING_PATHWAY, TNF_SIGNALING_PATHWAY, NF_KAPPA_B_SIGNALING_PATHWAY, JAK_STAT_SIGNALING_PATHWAY, CYTOKINE_CYTOKINE_RECEPTOR_INTERACTION, and NOD_LIKE_RECEPTOR_SIGNALING_PATHWAY (Fig. S2A). Collectively, these results indicate that TRIM36 positively promotes TLR4 signaling pathway activation to augment inflammatory responses.

TRIM36 directly interacts with TAK1 through an extensive multi-domain interface

As TRIM36 is a member of the TRIM family, which often functions by binding to target molecules and mediating their ubiquitination to regulate their activity[9, 18], we hypothesized that TRIM36 might exert its effect by interacting with key components of the TLR4 signaling pathway, given that its knockout significantly inhibits TLR4 pathway activation. To test this, we employed an ectopic expression system in HEK293T cells to investigate potential interactions between TRIM36 and several critical molecules within the TLR4 pathway (TAK1, TRAF6, TAB1, TAB2, and MYD88). The results confirmed that TRIM36 specifically interacted with TAK1 (Fig. S3A). TAK1 functions as a master regulatory kinase in signal transduction cascades, critically orchestrating TLR4 signaling pathway activation through phosphorylation-dependent mechanisms[33]. To further validate this interaction, we examined the functional relationship between TRIM36 and TAK1 in both HEK293T cells and BMDMs. Co-immunoprecipitation (Co-IP) assays demonstrated a robust interaction, evident upon exogenous expression in HEK293T cells and, more importantly, under physiological conditions between the endogenous proteins in BMDMs (Fig. 4A, B).

To map the specific interaction domains, we performed Co-IP assays in HEK293T cells using a series of truncation mutants. Assays between full-length TAK1 and TRIM36 truncation mutants revealed that the RING and SPRY domains of TRIM36 are primarily responsible for the interaction (Fig. 4C). Similarly, reciprocal Co-IP using TAK1 truncation mutants and full-length TRIM36 demonstrated an extensive binding interface, indicating that multiple domains of TAK1 contributed to the binding (Fig. 4D). Molecular docking simulations further supported a model of extensive, multi-domain interaction between TRIM36 and TAK1, rather than binding mediated by a single, localized site or fragment (Fig. S4A). Collectively, these data delineate a direct and extensive interaction between TRIM36 and TAK1, providing a structural basis for the ensuing functional regulation.

TRIM36 drives pro-inflammatory signaling via K63-ubiquitination and activation of TAK1

Having established the physical interaction between TRIM36 and TAK1, we next asked whether TRIM36 mediates the ubiquitination of TAK1. Upon co-expression in HEK293T cells, TRIM36 enhanced TAK1 ubiquitination in a dose-dependent manner (Fig. 5A). This effect was confirmed under physiological conditions, as TRIM36 deficiency significantly attenuated TAK1 ubiquitination in BMDMs (Fig. 5B). To ascertain the specificity of this effect, we generated a RING domain-deleted TRIM36 mutant (ΔRING) and found that it failed to promote TAK1 ubiquitination, demonstrating that TRIM36 acts as a bona fide E3 ligase for TAK1 in a RING-dependent manner (Fig. 5C).

We next determined the linkage specificity of TRIM36-mediated ubiquitination. Immunoblotting with linkage-specific antibodies revealed that TRIM36 predominantly catalyzed K63-linked polyubiquitination of TAK1, a finding consistent between HEK293T cells and BMDMs (Fig. 5D, E). To pinpoint the specific acceptor site, we generated lysine-to-arginine point mutants at TAK1 positions 34, 158, 209, and 562 – residues selected based on prior reports of potential K63-linked ubiquitination sites[34]. Among these, the K158R mutation caused a marked reduction in ubiquitination, conclusively identifying lysine 158 as the primary site for TRIM36-mediated K63-linked ubiquitination on TAK1 (Fig. 5F).

To functionally validate that TRIM36 potentiates TLR4-induced inflammatory responses through TAK1, we overexpressed TRIM36 in wild-type BMDMs and simultaneously knocked down TAK1. Overexpression of TRIM36 alone markedly enhanced LPS-induced phosphorylation of downstream signaling components (TAK1, IκBα, and p65) and the secretion of pro-inflammatory mediators (IL-1β, IL-6, TNF-α, and NO). Notably, knockdown of TAK1 by siRNA completely abrogated the TRIM36-mediated enhancement of IL-1β and IL-6 secretion, whereas the elevated levels of TNF-α and NO were only partially attenuated and remained significantly higher than the control group (Fig. 6B). Despite this partial effect on TNF-α and NO, the overall data demonstrate that TRIM36 critically depends on TAK1 to drive the majority of its pro-inflammatory program, with IL-1β and IL-6 being strictly TAK1-dependent. Collectively, these results indicate that TRIM36 functions as an upstream activator of TAK1, and that the TRIM36-TAK1 axis is a primary mediator of TRIM36-induced hyperinflammation.

TRIM36 potentiates inflammatory responses in human THP-1 Mφ and correlates with sepsis severity

To further validate the pro-inflammatory role of TRIM36 in sepsis, we employed human THP-1-derived macrophages (THP-1 Mφ) and performed TRIM36 knockdown followed by LPS stimulation (Fig. 7A). Consistently, reduced activation of the TLR4 signaling pathway was observed upon TRIM36 knockdown, as indicated by decreased phosphorylation levels of TAK1, IκBα, and p65 (Fig. 7B). We next measured the levels of pro-inflammatory mediators (IL-1β, IL-6, TNF-α, and NO) in the culture supernatants and found that TRIM36 knockdown led to significantly lower secretion of these mediators (Fig. 7C). Interrogation of the public transcriptomic database GEO (dataset GSE54514) revealed that TRIM36 transcript levels were significantly higher in non-survivors of sepsis than in survivors (Fig. 7D). Collectively, these findings further support a pro-inflammatory role for TRIM36 in human sepsis, wherein its elevated expression is associated with poor patient outcomes. Targeting TRIM36 may therefore represent a novel therapeutic strategy for sepsis.

Discussion

In this study, we identified TRIM36 as a previously unrecognized critical positive regulator of hyperinflammation in sepsis (Fig. 7E). We found that LPS stimulation robustly upregulated TRIM36 expression in macrophages and that genetic ablation of *Trim36* in vivo or its knockdown in vitro effectively attenuated systemic inflammatory responses and cytokine hypersecretion. Mechanistically, we found that TRIM36 directly interacted with TAK1 and catalyzed its K63-linked ubiquitination at lysine 158, a prerequisite for full activation of the TAK1–IκBα–NF-κB signaling axis. Collectively, our findings from cellular models, animal studies, and human data analysis establish TRIM36 as a novel and potent amplifier of TLR4 signaling and a promising therapeutic target for sepsis.

TAK1 is a master regulator that sits atop multiple inflammatory cascades, and its activity is tightly controlled by various post-translational modifications[7]. Although K63-linked ubiquitination is known to be crucial for TAK1 activation, the specific E3 ubiquitin ligases that mediate this modification in the context of TLR4 signaling and sepsis have remained incompletely defined[34]. Our work directly addresses this knowledge gap by identifying TRIM36 as the essential E3 ligase responsible for TAK1 ubiquitination and activation upon LPS challenge. The specificity of this interaction is highlighted by our findings that TRIM36 binds TAK1, but not other key components such as TRAF6, TAB1, TAB2, or MYD88, and that its RING domain is indispensable for its catalytic activity. This places TRIM36 as a dedicated and non-redundant regulator of TAK1. Furthermore, our precise mapping of the ubiquitination site to lysine 158 (K158) on TAK1 provides a molecularly defined mechanism for TRIM36-dependent signaling amplification. The extensive, multi-domain interaction between TRIM36 and TAK1, supported by our molecular docking data, suggests the formation of a stable complex that ensures efficient and specific ubiquitination.

Our findings are consistent with the emerging role of TRIM family proteins as pivotal modulators of innate immunity and inflammatory pathways[18]. Several TRIM members have been reported to regulate TLR signaling, albeit often with divergent and context-dependent functions. For example, some TRIM proteins act as negative regulators by targeting signaling components for degradation[20, 22], whereas others, such as TRIM36, serve as positive amplifiers. Our study adds a crucial layer to this understanding by delineating a clear mechanism: TRIM36-mediated K63-linked ubiquitination directly activates TAK1. The clinical relevance of this mechanism is strongly supported by our analysis of human transcriptomic data, which revealed a significant association between elevated TRIM36 levels and mortality in patients with sepsis. This correlation suggests that the TRIM36–TAK1 axis is not merely a mechanistic finding in mice but is also operational and pathologically significant in human disease.

The functional consequences of disrupting the TRIM36–TAK1 axis are profound. Trim36 deficiency led to a marked attenuation of the systemic inflammatory response in vivo, as evidenced by improved survival, mitigated hypothermia, reduced lung injury, and decreased levels of pro-inflammatory cytokines in both bronchoalveolar lavage fluid (BALF) and serum. At the cellular level, *Trim36*$^{-/-}$ macrophages exhibited a blunted response to LPS, characterized by diminished phosphorylation of TAK1, IκBα, and p65, and a failure to fully polarize towards a pro-inflammatory M1 phenotype. The rescue of the inflammatory phenotype upon TAK1 overexpression in *Trim36*$^{-/-}$ macrophages provides direct functional evidence that TAK1 is the primary downstream effector of TRIM36. This places TRIM36 upstream of a critical bottleneck in the inflammatory signaling network, making it an attractive target for therapeutic intervention.

Our functional rescue experiments revealed a notable divergence in the TAK1 dependency of different pro-inflammatory mediators induced by TRIM36. Whereas TRIM36-mediated IL-1β and IL-6 production was completely abrogated upon TAK1 knockdown, TNF-α and NO secretion was only partially attenuated and remained significantly elevated in the absence of TAK1 (Fig. 6B). This observation suggests that TRIM36 may engage multiple downstream signaling axes. It is well documented that IL-1β and IL-6 are canonical NF-κB target genes whose expression is tightly coupled to the TAK1-IKK-NF-κB pathway. In contrast, TNF-α and iNOS (the enzyme responsible for NO production) can also be regulated by alternative mechanisms, including AP-1-mediated transcription and the JAK-STAT pathway[35–37]. Therefore, while the TRIM36-TAK1 axis constitutes a major pathway driving hyperinflammation, additional TAK1-independent mechanisms may contribute to the full spectrum of TRIM36-mediated inflammatory responses. Future studies aimed at identifying other ubiquitination targets of TRIM36 will be necessary to fully understand its regulatory network.

One limitation of our study is the primary use of an LPS-induced endotoxemia model. Future work using polymicrobial models, such as cecal ligation and puncture (CLP), would strengthen the clinical relevance of our findings. An additional important aspect for future investigation concerns the temporal dynamics of TRIM36 expression and function across different phases of sepsis.

In conclusion, our study unveils a novel and sophisticated mechanism of inflammatory regulation in sepsis. We identify TRIM36 as an essential E3 ligase that orchestrates the activation of the TAK1–IκBα–NF-κB pathway through K63-linked ubiquitination, thereby driving the hyperinflammatory response that characterizes early sepsis. The combination of mechanistic depth, validation in human data, and demonstration of efficacy in preclinical models highlights the translational potential of our findings. Targeting the TRIM36–TAK1 interaction interface or the catalytic activity of TRIM36 represents a promising therapeutic strategy for precision anti-inflammatory therapy in sepsis.

Materials and methods

Mice

Trim36$^{-/-}$ mice and their *Trim36*$^{+/+}$ littermate controls on a C57BL/6 background were generated by Cyagen Biosciences (Suzhou, China). All mice were maintained under specific pathogen-free (SPF) conditions and were used at 6–12 weeks of age. Group assignment was randomized. All mice were all C57BL/6 background and maintained in the Lab Animal Center of Guangzhou Medical University under specific pathogen-free conditions. All animal experiments were conducted in accordance with protocols approved by the Medical Ethics Board and the Biosafety Management Committee of Guangzhou Medical University. All mice were used at an age of 6–12 weeks and were randomly divided into different groups.

LPS-induced sepsis model

Male mice were used in the animal model to avoid the potential influence of estrogen on survival and inflammation during sepsis. LPS (L4516, Sigma-Aldrich, 10 mg/kg) was administered intraperitoneally to induce endotoxemia. Eight-week-old male *Trim36*$^{+/+}$ and *Trim36*$^{-/-}$ mice were euthanized by CO_2 inhalation 24 h after LPS injection, and samples were collected for measurement of inflammatory mediators.

Bronchoalveolar lavage fluid (BALF) collection

BALF was obtained by cannulating the trachea, followed by lavage with 1 mL of ice-cold PBS. The PBS was instilled and withdrawn three times, and the final lavage fluid was collected for subsequent analysis.

Histological analysis

Lung lobes were fixed in 4% paraformaldehyde, embedded in paraffin, and sectioned. The sections were then stained with hematoxylin and eosin (H&E) for assessment of pathological inflammatory infiltration.

Isolation of peritoneal macrophages

Peritoneal macrophages were harvested by intraperitoneal injection of 5 mL of ice-cold complete RPMI-1640 medium. After gentle abdominal massage for 3 min, the lavage fluid was aspirated. Cells were pelleted by centrifugation at 500 × g for 3 min and washed once with 1 mL of PBS prior to flow cytometry staining.

Flow cytometry for surface marker staining

Peritoneal macrophages were stained for surface markers with anti-mouse F4/80-BG Violet450 (02922-40-100, BioGems), anti-mouse CD11b-PE (03221-60-100, BioGems), anti-mouse CD80-PE-Cy5 (MA5-28657, Invitrogen), and anti-mouse CD86-APC (08912-80-100, BioGems). Cells were incubated with appropriately titrated antibodies in staining buffer at 4°C for 30 min. After incubation, the cells were washed and resuspended in fresh staining buffer prior to acquisition. Flow cytometry was performed on a Beckman CytoFLEX S flow cytometer, and data were analyzed using FlowJo software (version 10.8.1).

Cell culture

HEK293T and THP-1 cell lines were obtained from the American Type Culture Collection (ATCC). HEK293T cells were maintained in Dulbecco's modified Eagle's medium (DMEM; Corning, USA), and THP-1 cells were cultured in RPMI-1640 medium (Corning, USA), both supplemented with 10% fetal bovine serum (FBS; Corning, USA). Bone marrow-derived macrophages (BMDMs) were isolated from 6- to 8-week-old C57BL/6 mice under aseptic conditions. Precursor cells were differentiated in DMEM containing 10% FBS and 40 ng/mL macrophage colony-stimulating factor (M-CSF) at 37°C with 5% CO_2. The medium was replenished with fresh M-CSF (40 ng/mL; Novoprotein, China)-containing medium on days 3 and 5. Differentiated BMDMs were ready for experimentation by day 7.

Induction of THP-1-derived macrophages (THP1-Mφ)

THP-1 cells were differentiated into M0 macrophages by treatment with 25 ng/mL phorbol 12-myristate 13-acetate (PMA) in RPMI-1640 complete medium (supplemented with 10% FBS) for 5 days. Following differentiation, the cells were washed three times with PBS and subsequently rested in PMA-free complete medium for 24 h prior to subsequent experiments.

Adenoviral overexpression and siRNA transfection

Adenoviruses for overexpressing TRIM36 (Ad-*Trim36*) and the corresponding control virus (Ad-Ctrl) were obtained from HanYi Biotech. Knockdown or overexpression experiments were performed according to the manufacturer's instructions. siRNAs targeting Tak1 (si*Tak1*) and a negative control siRNA (siNegative) were purchased from Tsingke Biotech.

For adenovirus-mediated overexpression, cells in six-well plates were infected at a multiplicity of infection (MOI) of 150. The viral infection was performed in 1 mL of complete DMEM containing the appropriate volume of adenovirus stock and Polybrene. After gentle mixing, the virus-containing medium was added to the cells. Following incubation for 6–8 h, the medium was replaced with fresh complete DMEM. The cells were then cultured for an additional 24 h prior to further experiments.

For siRNA-mediated knockdown, the transfection procedure was as follows: Solution A was prepared by mixing 80 nM siRNA with 250 µL of Opti-MEM medium (31985070, Gibco) and incubating at room temperature for 10 min. Solution B was prepared by diluting 10 µL of Lipofectamine RNAiMAX (13778030, Invitrogen) in 250 µL of Opti-MEM medium, followed by incubation at room temperature for

10 min. Solution C was then formed by combining Solutions A and B and incubating the mixture at room temperature for an additional 10 min. Subsequently, 500 μL of Solution C was added to cells seeded in six-well plates. The total volume was adjusted to 1 mL with Opti-MEM. After incubation in the CO_2 incubator for 6–8 h, the transfection mixture was removed, and the cells were washed three times with PBS. Fresh complete RPMI-1640 medium was then added, and the cells were cultured for another 24 h before subsequent stimulation experiments.

Plasmid constructs and transfection

The following expression vectors were generated by inserting synthesized complementary DNAs into the pcDNA3.1 vector (Sangon Biotech, China): pcDNA3.1-*Trim36*-3×FLAG, pcDNA3.1-*Tak1*-HA, pcDNA3.1-*Traf6*-HA, pcDNA3.1-*Tab1*-HA, pcDNA3.1-*Tab2*-HA, pcDNA3.1-*Myd88*-HA, pcDNA3.1-Ub-V5, pcDNA3.1-Δ-RING-*Trim36*-FLAG, pcDNA3.1-*Trim36*(1-345)-FLAG, pcDNA3.1-*Trim36*(155-345)-HA, pcDNA3.1-*Trim36*(207-345), pcDNA3.1-*Trim36*(271-728)-FLAG, pcDNA3.1-*Trim36*(511-728), pcDNA3.1-*Tak1*(1-300)-HA, pcDNA3.1-*Tak1*(301-579), pcDNA3.1-*Tak1*(K34R)-HA, pcDNA3.1-*Tak1*(K158R)-HA, pcDNA3.1-*Tak1*(209R)-HA, pcDNA3.1-*Tak1*(K562R)-HA, pcDNA3.1-K0-Ub-V5, pcDNA3.1-K6-Ub-V5, pcDNA3.1-K11-Ub-V5, pcDNA3.1-K27-Ub-V5, pcDNA3.1-K33-Ub-V5, pcDNA3.1-K48-Ub-V5, and pcDNA3.1-K63-Ub-V5. All plasmids were sequenced to confirm the presence of the designed mutations without any unintended alterations. Plasmids of the indicated quality and quantity were transfected into the indicated cells using PEI (Sigma-Aldrich, USA) according to the manufacturer's instructions.

RNA extraction and quantitative real-time PCR

BMDMs were lysed with 1 mL of TRIzol Reagent (Thermo Fisher Scientific, USA) for total RNA isolation. RNA concentration and purity were analyzed using a Nanodrop 2000c Spectrophotometer (Thermo Fisher Scientific, USA). Equal amounts of RNA were then reverse-transcribed into cDNA using the TransScript Uni All-in-One First-Strand cDNA Synthesis SuperMix Kit (TransGen Biotech, China). The relative mRNA levels of target genes were quantified by qPCR using the TransStart Top Green qPCR SuperMix kit (TransGen Biotech, China) on a LightCycler96 (Roche, Switzerland). Actb (encoding β-actin) was used as an endogenous reference for normalization. Data were analyzed using the $2^{-\Delta\Delta CT}$ method. Primer sequences are listed in Supplementary Table 1.

Western blot

Cells were washed three times with ice-cold PBS and then lysed in lysis buffer [20 mM HEPES (pH 7.9), 10 mM KCl, 1 mM EDTA, 400 mM NaCl, 0.5% NP-40, and 5% glycerol] containing 1/10 volume of Phosphatase Inhibitor Cocktail (Roche, Switzerland) and 1 mM dithiothreitol (DTT; Sigma-Aldrich, USA). Protein concentrations were quantified using the Quick Start Bradford Dye Reagent (Bio-Rad, USA). Protein samples were denatured at 95°C for 10 min, separated by SDS-polyacrylamide gel electrophoresis (SDS-PAGE), and transferred to a polyvinylidene difluoride (PVDF) membrane (Merck Millipore, Germany). The membrane was blocked in 5% bovine serum albumin (BSA; Sigma-Aldrich, USA) for 1 h at room temperature and then incubated overnight at 4°C with rotation with the primary

antibodies listed below: TRIM36 (Proteintech, 25913-1-AP), β-actin (Trans, HC201), GAPDH (Proteintech, 60004-1-Ig), p65 (CST, 4764S), phospho-p65 (CST, 3033S), TBK1 (CST, 3013S), phospho-TBK1 (CST, 5483S), IRF3 (CST, 4302), phospho-IRF3 (CST, 79945), AKT (CST, 4691S), phospho-AKT (CST, 4060S), JNK (CST, 9252S), phospho-JNK (CST, 9251S), p38 (CST, 2307S), phospho-p38 (CST, 4511S), TAK1 (Abclonal, A19077), phospho-TAK1 (Abclonal, A9437), IκBα (Abclonal, A19714), phospho-IκBα (Abclonal, AP0707), ubiquitin (Proteintech, 10201-2-AP), K63-linkage-specific polyubiquitin (CST, 5621), HA tag (Abclonal, AE105), FLAG tag (MBL, M185-3L), and V5 tag (Immunoway, YM3005). The membranes were then incubated with appropriate horseradish peroxidase (HRP)-conjugated secondary antibodies [goat anti-mouse IgG (H + L), 31430; goat anti-rabbit IgG $F(ab')_2$, 31234; Thermo Fisher Scientific] for 1 h at room temperature and visualized using Plus-ECL (FDbio Science, China) according to the manufacturer's protocol.

Co-immunoprecipitation (Co-IP) assay

Whole-cell extracts were harvested 48 h after transfection and lysed in immunoprecipitation (IP) buffer [1% (v/v) NP-40, 1.5 M Tris-HCl (pH 8.8), 0.5 M EDTA, 5 M NaCl, and protease inhibitors (Roche, Switzerland)]. The lysates were subsequently sonicated for 10 min at 4°C using an ultrasound disruptor (Diagenode Bioruptor, Belgium), followed by centrifugation at 12,000 rpm (revolutions per minute) for 10 min at 4°C. The resulting supernatant was quantified for protein content, yielding approximately 1 mg of protein. The protein sample was then incubated with 2 μg of the respective antibody overnight at 4°C. Subsequently, the protein-antibody complexes were incubated with Protein A/G magnetic beads (MCE, China) for 1–2 h. The beads were then washed five times with IP buffer (1× PBS containing 0.5% Tween-20, pH 7.4). For immunoblotting, immunoprecipitants or whole-cell lysates were eluted with SDS sample buffer by boiling for 5 min. The resulting samples were then subjected to SDS-PAGE, transferred onto nitrocellulose membranes, and blotted with the indicated antibodies.

Enzyme linked immunosorbent assay

Cytokine concentrations in serum and cell culture supernatants were measured using mouse IL-1β, IL-6, and TNF-α ELISA kits (MultiScience, China) according to the manufacturer's instructions. For serum collection, peripheral blood samples from mice were obtained by eyeball extirpation and allowed to clot for 30 min at room temperature, followed by centrifugation at 3000 rpm for 10 min. Cell culture supernatants were harvested from infected cells and used for cytokine analysis.

Griess assay

A Cells were cultured overnight in 12-well plates (5×10^5 cells per well, 1 mL of medium per well) and then treated with LPS for the indicated times. Culture supernatants were collected and used to measure nitric oxide (NO) production. NO levels were determined using a commercial Griess assay kit (Promega, USA) according to the manufacturer's instructions. Briefly, 50 μL of cell culture supernatant was mixed with 50 μL of sulfanilamide solution and incubated at room temperature for 10 min in the dark. Then, 50

μL of NED solution was added, followed by incubation at room temperature for another 10 min. Absorbance was measured at 520 nm using a microplate reader.

Molecular docking simulation

The three-dimensional structures of TRIM36 and TAK1 in PDB format were retrieved from the AlphaFold models provided by the UniProt database (https://www.uniprot.org). Protein–protein docking was performed using the HDOCK server (http://hdock.phys.hust.edu.cn) with default parameters, with TRIM36 set as the receptor and TAK1 as the ligand. Structural visualization and annotation of key interacting residues and hydrogen bonds were carried out using PyMOL (The PyMOL Molecular Graphics System).

Statistics

All experiments were performed at least three times, and data are presented as mean ± SD. When multiple samples were used, they represented biological replicates of mice randomly assigned to each experimental group, rather than technical replicates. No blinding was performed during the animal experiments. Statistical analysis was performed using Prism 9 (GraphPad Software). Unpaired two-tailed Student's t-tests were used to compare two groups with similar variances. Statistical significance was defined as a *P* value of less than 0.05.

Declarations

Acknowledgments

This work was funded by grants from National Natural Science Foundation of China (82471780 awarded to S.H.F.); Zhongshan's Third Batch of Social Welfare and Basic Research Projects (2023B3024 awarded to K.C.); the Science and Technology Fund of Guangdong Provincial Hospital of Chinese Medicine (YN2024GZRPY048 awarded to S.H.W.); the Research Fund of Health Commission of Guangdong Province (A2023130 awarded to Y.J.K., B2023141 awarded to S.H.W.); Zhongshan Scientific Research Special Project for the Inheritance and Innovative Development of Traditional Chinese Medicine (2024B3008 awarded to K.C.); Fund of the State Key Laboratory of Respiratory Diseases (SKLRD-Z-202506 awarded to S.H.F.). We thank all members of Shengfeng Hu' Lab for helpful discussions and input.

Author contributions

S.F.H., K.C., S.H.W., S.J.S., and D.N.N. designed research; S.J.S., D.N.N., Z.A., Y.L.F., S.W.W., J.L.S., H.R.H., X.L.Y., Q.L., X.D.Y., W.H.L., and W.L. conducted research; S.J.S., D.N.N., Z.A., K.C., S.H.W., and S.F.H. analyzed data; S.J.S., D.N.N., Z.A., and S.F.H. wrote the paper; S.F.H., K.C., and S.H.W. provided essential reagents, or provided essential materials; S.F.H., K.C., and S.H.W. as the corresponding author conducted the experiment. All authors read and approved the final manuscript.

Conflict of Interest

The authors declare no competing financial interests.

Data and materials availability

All data needed to evaluate the conclusions in the paper are present in the paper and/or the Supplementary Materials.

References

1. Cecconi M, Evans L, Levy M, Rhodes A. Sepsis and septic shock. Lancet. 2018;392:75–87.
2. Nedeva C, Menassa J, Puthalakath H. Sepsis: Inflammation Is a Necessary Evil. Front Cell Dev Biol. 2019;7:108.
3. Chen S, Zhang C, Luo J, Lin Z, Chang T, Dong L, et al. Macrophage activation syndrome in Sepsis: from pathogenesis to clinical management. Inflamm Res. 2024;73:2179–97.
4. Gong T, Liu L, Jiang W, Zhou R. DAMP-sensing receptors in sterile inflammation and inflammatory diseases. Nat Rev Immunol. 2020;20:95–112.
5. Fitzgerald KA, Kagan JC. Toll-like Receptors and the Control of Immunity. Cell. 2020;180:1044–66.
6. Guo Q, Jin Y, Chen X, Ye X, Shen X, Lin M, et al. NF-κB in biology and targeted therapy: new insights and translational implications. Signal Transduct Target Ther. 2024;9:53.
7. Ninomiya-Tsuji J, Kishimoto K, Hiyama A, Inoue J, Cao Z, Matsumoto K. The kinase TAK1 can activate the NIK-I kappaB as well as the MAP kinase cascade in the IL-1 signalling pathway. Nature. 1999;398:252–6.
8. Totzke J, Scarneo SA, Yang KW, Haystead TAJ. TAK1: a potent tumour necrosis factor inhibitor for the treatment of inflammatory diseases. Open Biol. 2020;10:200099.
9. Hatakeyama S. TRIM Family Proteins: Roles in Autophagy, Immunity, and Carcinogenesis. Trends Biochem Sci. 2017;42:297–311.
10. Ummanni R, Jost E, Braig M, Lohmann F, Mundt F, Barett C, et al. Ubiquitin carboxyl-terminal hydrolase 1 (UCHL1) is a potential tumour suppressor in prostate cancer and is frequently silenced by promoter methylation. Mol Cancer. 2011;10:129.
11. Foot N, Henshall T, Kumar S. Ubiquitination and the Regulation of Membrane Proteins. Physiol Rev. 2017;97:253–81.
12. Zheng N, Shabek N. Ubiquitin Ligases: Structure, Function, and Regulation. Annu Rev Biochem. 2017;86:129–57.
13. Akutsu M, Dikic I, Bremm A. Ubiquitin chain diversity at a glance. J Cell Sci. 2016;129:875–80.
14. Popovic D, Vucic D, Dikic I. Ubiquitination in disease pathogenesis and treatment. Nat Med. 2014;20:1242–53.
15. Mukhopadhyay D, Riezman H. Proteasome-independent functions of ubiquitin in endocytosis and signaling. Science. 2007;315:201–5.

16. Tracz M, Bialek W. Beyond K48 and K63: non-canonical protein ubiquitination. Cell Mol Biol Lett. 2021;26:1.
17. Ohtake F, Tsuchiya H, Saeki Y, Tanaka K. K63 ubiquitylation triggers proteasomal degradation by seeding branched ubiquitin chains. Proc Natl Acad Sci U S A. 2018;115:E1401–8.
18. Ozato K, Shin DM, Chang TH, Morse HC. TRIM family proteins and their emerging roles in innate immunity. Nat Rev Immunol. 2008;8:849–60.
19. Huang B, Baek SH. Trim13 Potentiates Toll-Like Receptor 2-Mediated Nuclear Factor κB Activation via K29-Linked Polyubiquitination of Tumor Necrosis Factor Receptor-Associated Factor 6. Mol Pharmacol. 2017;91:307–16.
20. Shi M, Deng W, Bi E, Mao K, Ji Y, Lin G, et al. TRIM30 alpha negatively regulates TLR-mediated NF-kappa B activation by targeting TAB2 and TAB3 for degradation. Nat Immunol. 2008;9:369–77.
21. Yang Q, Liu TT, Lin H, Zhang M, Wei J, Luo WW, et al. TRIM32-TAX1BP1-dependent selective autophagic degradation of TRIF negatively regulates TLR3/4-mediated innate immune responses. PLoS Pathog. 2017;13:e1006600.
22. Hu MM, Yang Q, Zhang J, Liu SM, Zhang Y, Lin H, et al. TRIM38 inhibits TNFα- and IL-1β-triggered NF-κB activation by mediating lysosome-dependent degradation of TAB2/3. Proc Natl Acad Sci U S A. 2014;111:1509–14.
23. Shen Y, Li NL, Wang J, Liu B, Lester S, Li K. TRIM56 is an essential component of the TLR3 antiviral signaling pathway. J Biol Chem. 2012;287:36404–13.
24. Zhao W, Wang L, Zhang M, Wang P, Yuan C, Qi J, et al. Tripartite motif-containing protein 38 negatively regulates TLR3/4- and RIG-I-mediated IFN-β production and antiviral response by targeting NAP1. J Immunol. 2012;188:5311–8.
25. Kitamura K, Tanaka H, Nishimune Y. Haprin, a novel haploid germ cell-specific RING finger protein involved in the acrosome reaction. J Biol Chem. 2003;278:44417–23.
26. Mascaro M, Lages I, Meroni G. Microtubular TRIM36 E3 Ubiquitin Ligase in Embryonic Development and Spermatogenesis. Cells. 2022; 11.
27. Yu S, Li W, Liu X, Zhang H, Liu X, Zhang LW. TRIM36 enhances lung adenocarcinoma radiosensitivity and inhibits tumorigenesis through promoting RAD51 ubiquitination and antagonizing hsa-miR-376a-5p. Biochem Biophys Res Commun. 2022;628:1–10.
28. Liang C, Wang S, Qin C, Bao M, Cheng G, Liu B, et al. TRIM36, a novel androgen-responsive gene, enhances anti-androgen efficacy against prostate cancer by inhibiting MAPK/ERK signaling pathways. Cell Death Dis. 2018;9:155.
29. Liu X, Yan C, Chang C, Meng F, Shen W, Wang S, et al. FOXA2 Suppression by TRIM36 Exerts Anti-Tumor Role in Colorectal Cancer Via Inducing NRF2/GPX4-Regulated Ferroptosis. Adv Sci (Weinh). 2023;10:e2304521.
30. van der Poll T, Shankar-Hari M, Wiersinga WJ. The immunology of sepsis. Immunity. 2021;54:2450–64.

31. Fan Y, Mao R, Yang J. NF-κB and STAT3 signaling pathways collaboratively link inflammation to cancer. Protein Cell. 2013;4:176–85.
32. Yuan J, Dong X, Yap J, Hu J. The MAPK and AMPK signalings: interplay and implication in targeted cancer therapy. J Hematol Oncol. 2020;13:113.
33. Ajibade AA, Wang HY, Wang RF. Cell type-specific function of TAK1 in innate immune signaling. Trends Immunol. 2013;34:307–16.
34. Xu YR, Lei CQ. TAK1-TABs Complex: A Central Signalosome in Inflammatory Responses. Front Immunol. 2020;11:608976.
35. Rhoades KL, Golub SH, Economou JS. The regulation of the human tumor necrosis factor alpha promoter region in macrophage, T cell, and B cell lines. J Biol Chem. 1992;267:22102–7.
36. Zhang X, Liu Z, Li W, Kang Y, Xu Z, Li X, et al. MAPKs/AP-1, not NF-κB, is responsible for MCP-1 production in TNF-α-activated adipocytes. Adipocyte. 2022;11:477–86.
37. Tian L, Yin S, Wang J, Xiao H, Kuang T, Luo L, et al. Neutrophilic granule protein promotes lipopolysaccharide-induced iNOS/NO expression via JAK2/STAT1 signaling pathway and augments bacteria clearance of macrophages. Cell Mol Life Sci. 2025;82:385.

Figures

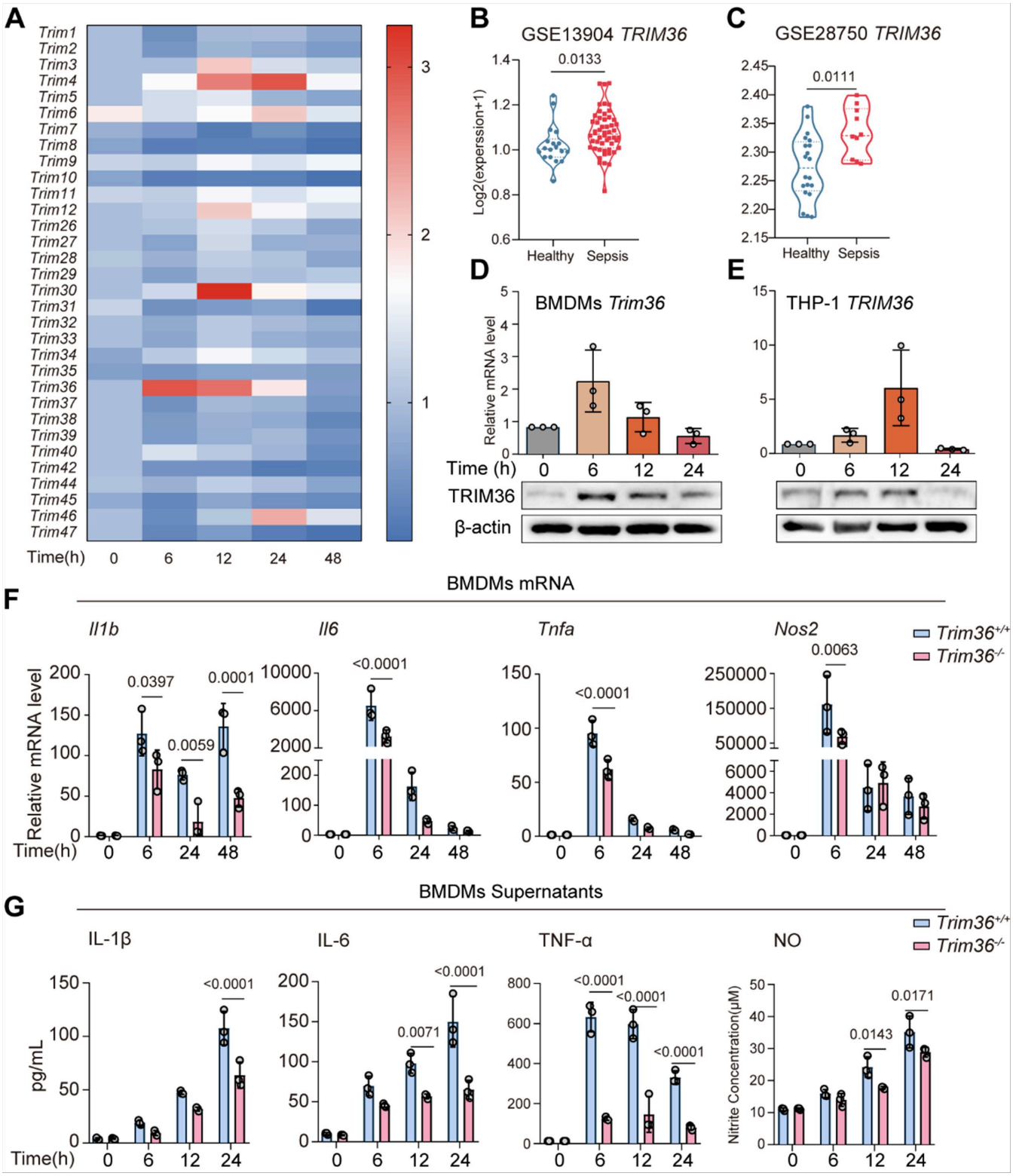


Figure 1

TRIM36 exerts a pro-inflammatory role in BMDMs. (A) Heatmap showing mRNA expression levels of TRIM family members in BMDMs treated with LPS (100 ng/mL) for different durations (n = 3). **(B, C)** Violin plots depicting the distribution of TRIM36 transcript levels in sepsis patients compared to healthy controls, analyzed from GEO datasets. (B: Healthy, n = 18; Sepsis, n = 52; and C: Healthy, n = 20; Sepsis, n = 10). **(D, E)** Time-dependent changes in Trim36 mRNA and protein expression in BMDMs and THP-1

cells following LPS (100 ng/mL) stimulation (n = 3). **(F, G)** Transcript levels and secretion of M1-type inflammatory cytokines (*Il1b*/IL-1β, *Il6*/IL-6, *Tnfa*/TNF-α, *Nos2*/NO) in LPS-stimulated BMDMs from *Trim36*$^{+/+}$ and *Trim36*$^{-/-}$ mice across various time points (n = 3). Data are presented as mean ± SD. Statistical significance was determined by the *Mann-Whitney U* test **(B, C)** and by two-way *ANOVA* with Sidak's post-hoc test **(F, G)**.

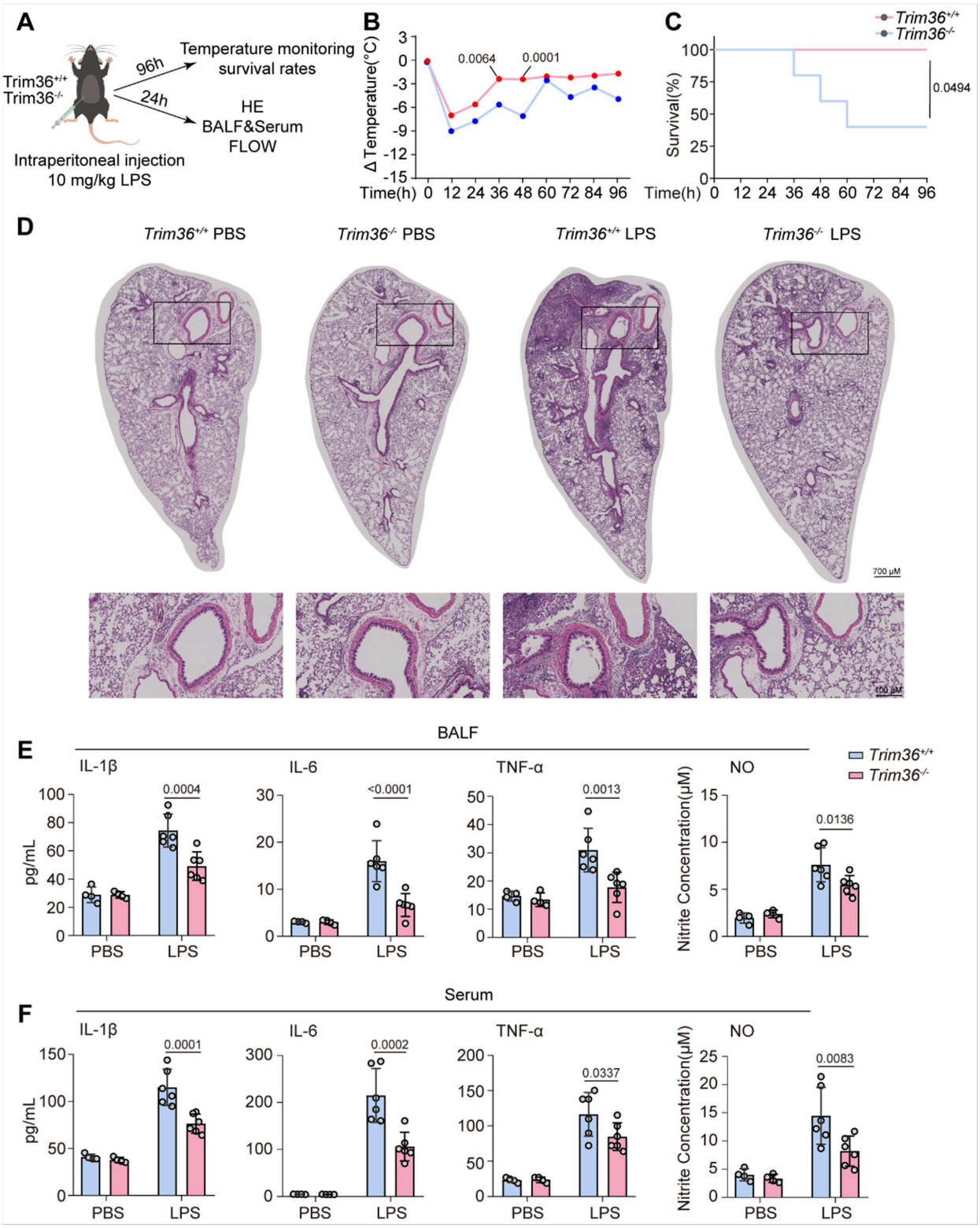


Figure 2

TRIM36 mediates sepsis progression in mice. (A) Schematic of the murine sepsis model induced by intraperitoneal injection of LPS (10 mg/kg). Body temperature and survival rate were monitored for 96 h, and inflammatory injury was assessed at 24 h. **(B)** Rectal temperature measurements of *Trim36*$^{+/+}$ and *Trim36*$^{-/-}$ mice every 12 h after LPS challenge (n = 5). **(C)** Comparative survival analysis of *Trim36*$^{+/+}$ and *Trim36*$^{-/-}$ mice over 96 h (n = 5). **(D)** Representative images of H&E-stained lung tissues from LPS-challenged mice. Scale bars, 700 μm (overview) and 100 μm (inset). **(E, F)** Quantitative analysis of IL-1β, IL-6, TNF-α, and NO levels in BALF **(E)** and serum **(F)** from mice at 24 h after LPS injection (n = 4-6). Data were presented as mean ± SD. Statistical analysis was performed by two-way *ANOVA* with Sidak's post-hoc test **(B)** or log-rank test **(C)**.

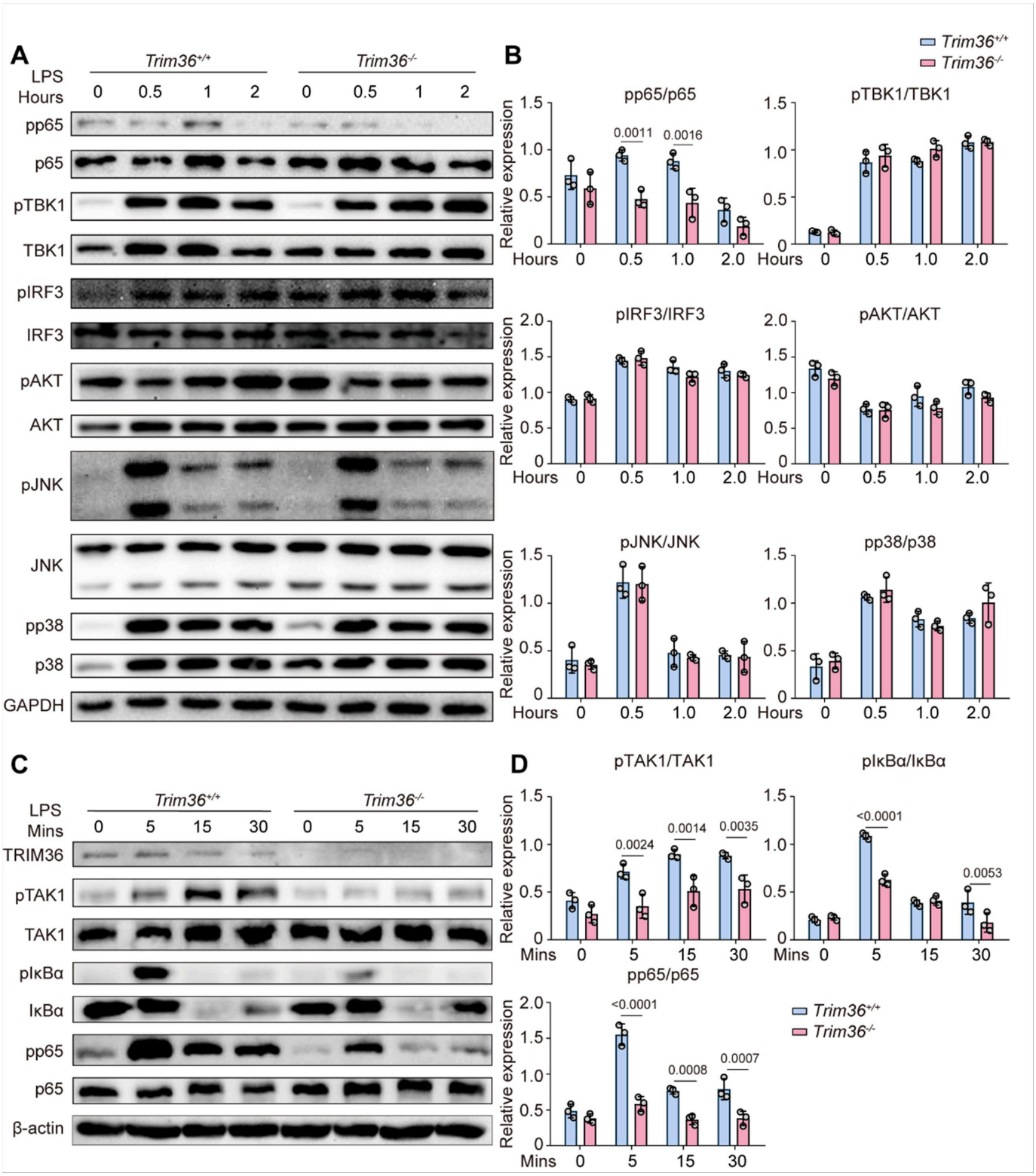


Figure 3

TRIM36 promotes the activation of the TLR4 signaling pathway in macrophages. (A, B) Time course of LPS-induced phosphorylation of key inflammatory signaling molecules in *Trim36*$^{+/+}$ and *Trim36*$^{-/-}$ BMDMs. Representative immunoblots **(A)** and corresponding quantification **(B)** of phosphorylated proteins are shown. Cells were stimulated with LPS (100 ng/mL) for the indicated times (n = 3). **(C, D)** Immunoblot analysis of TLR4 pathway components in *Trim36*$^{+/+}$ and *Trim36*$^{-/-}$ BMDMs upon brief LPS

stimulation. Representative images **(C)** and quantification **(D)** of protein expression levels at 0, 5, 15, and 30 minutes after LPS (100 ng/mL) treatment are shown (n = 3). Data are presented as mean ± SD. Statistical significance was determined by two-way *ANOVA* with Sidak's post-hoc test **(B, D)**.

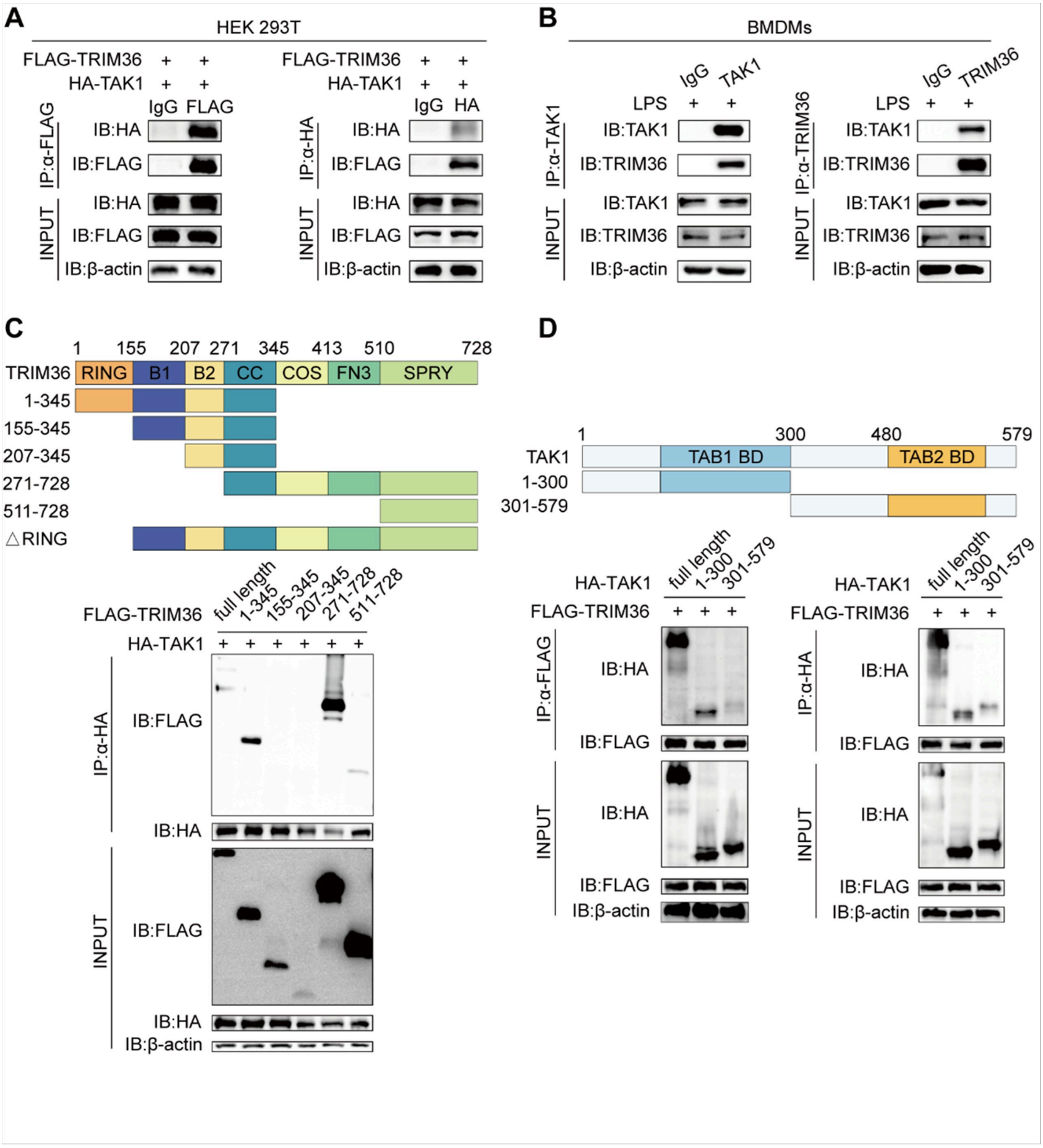


Figure 4

TRIM36 establishes an extensive interaction with TAK1. (A) Interaction between exogenous TRIM36 and TAK1 was analyzed by Co-IP in HEK 293T cells co-transfected with FLAG-TRIM36 and HA-TAK1. **(B)** Endogenous interaction between TRIM36 and TAK1 in BMDMs stimulated with LPS (100 ng/mL, 1 h) was determined by Co-IP. **(C, D)** Schematic diagrams of the domain structures of wild-type and deletion mutants of TRIM36 and TAK1. Mapping of the interacting domains between TRIM36 and TAK1 by Co-IP in HEK 293T cells expressing the indicated mutants.

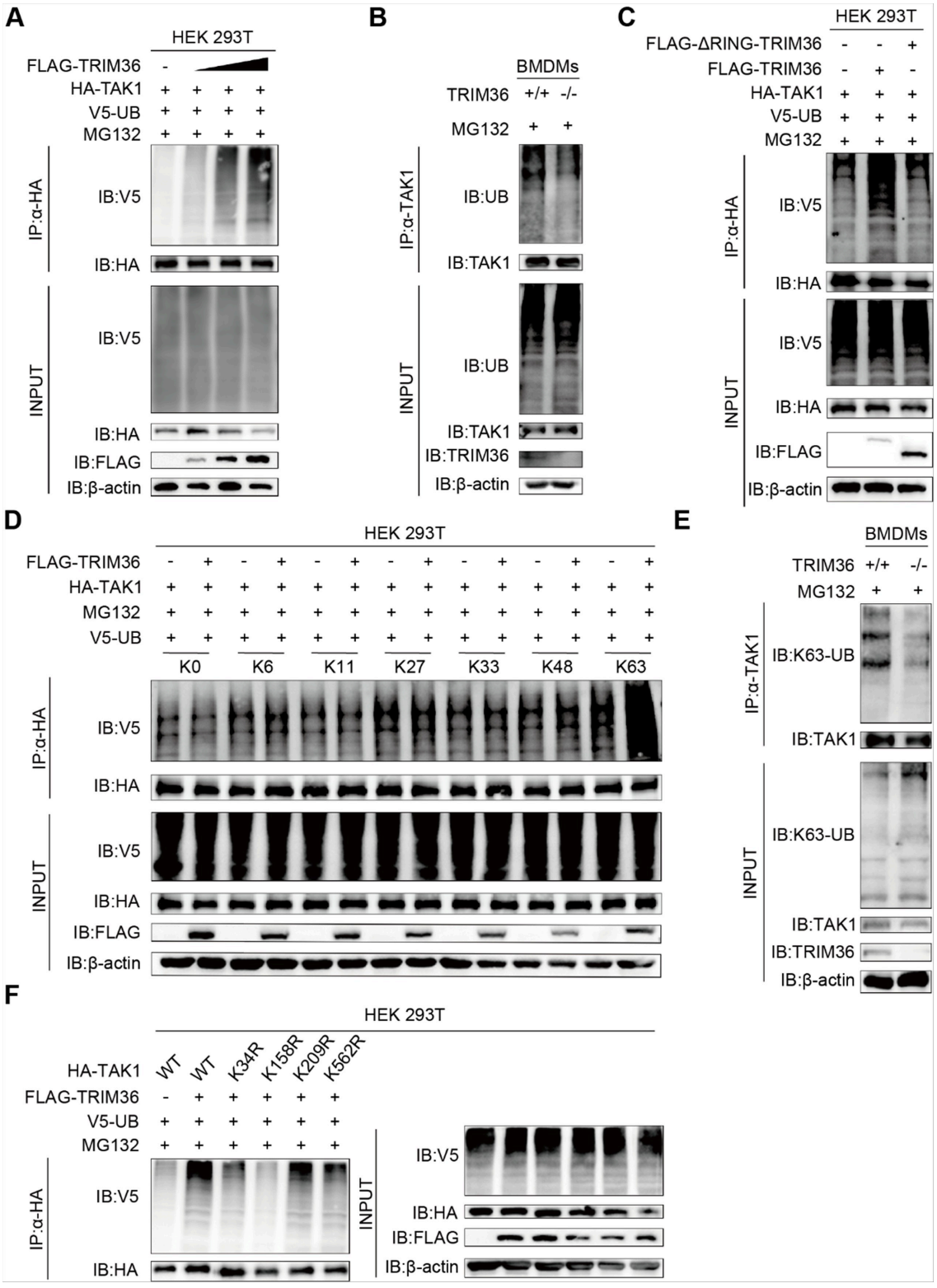


Figure 5

TRIM36 mediates specific K63-linked ubiquitination of TAK1 at K158. (A) TRIM36-mediated ubiquitination of TAK1 was examined in HEK 293T cells co-expressing FLAG-TRIM36, HA-TAK1, and V5-Ub and treated with MG132 (10 μM, 6 h). **(B)** LPS-induced ubiquitination of endogenous TAK1 was assessed in BMDMs from *Trim36*$^{+/+}$ and *Trim36*$^{-/-}$ mice by immunoprecipitation of TAK1 and immunoblotting for ubiquitin. **(C)** HEK 293T cells expressing HA-TAK1 and V5-Ub were co-transfected with vector, wild-type TRIM36, or the ΔRING mutant and treated with MG132 (10 μM, 6 h). **(D)** HEK 293T cells expressing FLAG-TRIM36, HA-TAK1, and wild-type V5-Ub or its linkage-specific mutants (K0, K6-only, K11-only, K27-only, K33-only, K48-only, K63-only) were treated with MG132 (10 μM, 6 h). **(E)** BMDMs isolated from *Trim36*$^{+/+}$ and *Trim36*$^{-/-}$ mice were stimulated with LPS (100 ng/mL) for 30 mins. **(F)** HEK 293T cells were co-transfected with FLAG-TRIM36, V5-Ub, and wild-type HA-TAK1 or its lysine-to-arginine mutants (K34R, K158R, K209R, K562R), followed by MG132 treatment (10 μM, 6 h).

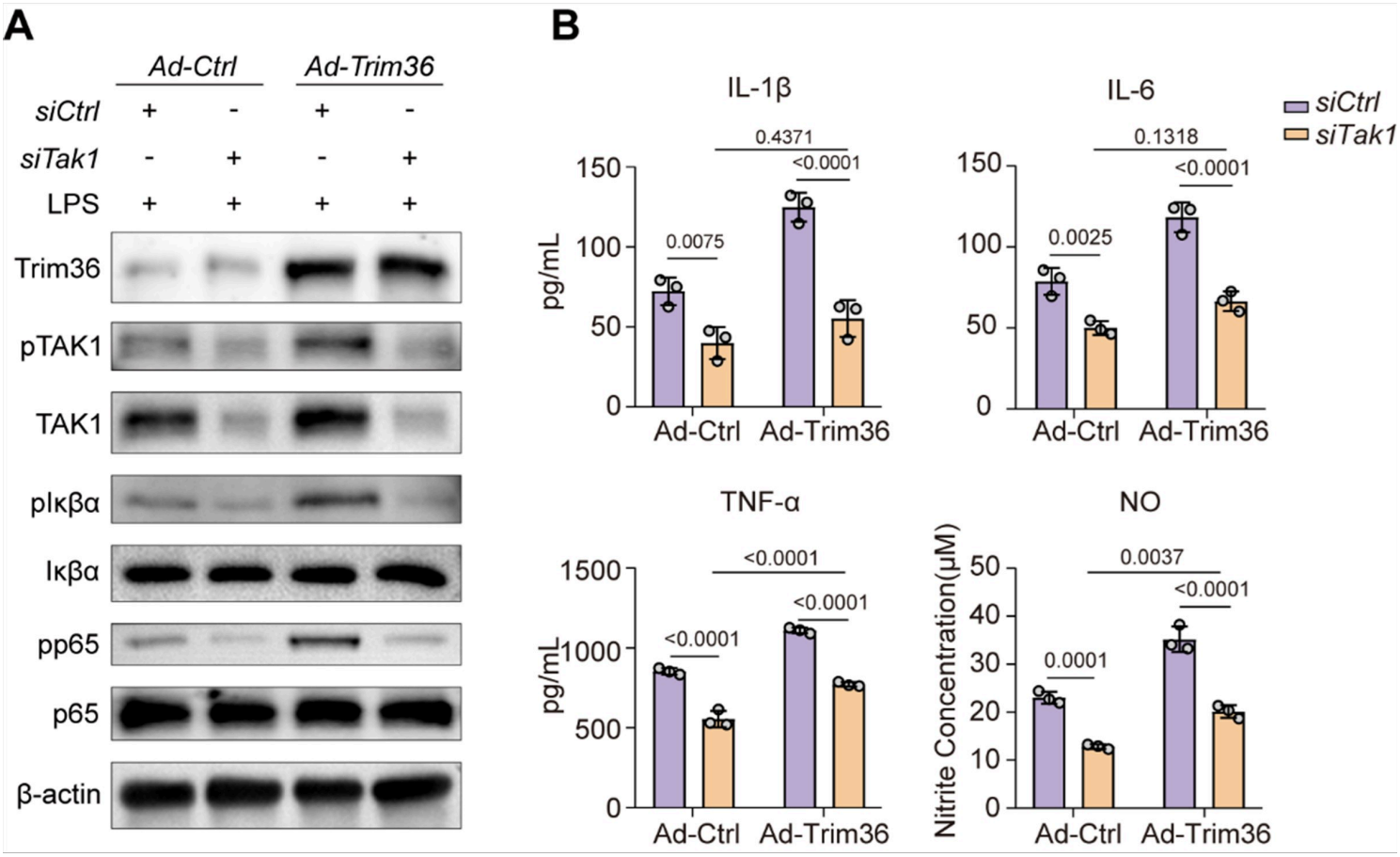


Figure 6

TRIM36 potentiates LPS-induced inflammatory signaling and cytokine production in a TAK1-dependent manner. (A) Western blot analysis of phosphorylated TAK1, IκBα, and p65 in wild-type (WT) BMDMs. Cells were transduced with Ad-Ctrl or Ad-*Trim36*for 24 h, followed by transfection with siCtrl or si*Tak1* for 24 h, and then stimulated with LPS (100 ng/mL) for 5 min. **(B)** ELISA of IL-1β, IL-6, TNF-α, and Griess Reagent System of NO levels in culture supernatants from BMDMs described in **(A)** after LPS stimulation

for 6 hours (n = 3). Data are presented as mean ± SD. Statistical significance was determined by two-way *ANOVA* followed by Sidak's multiple comparisons test.

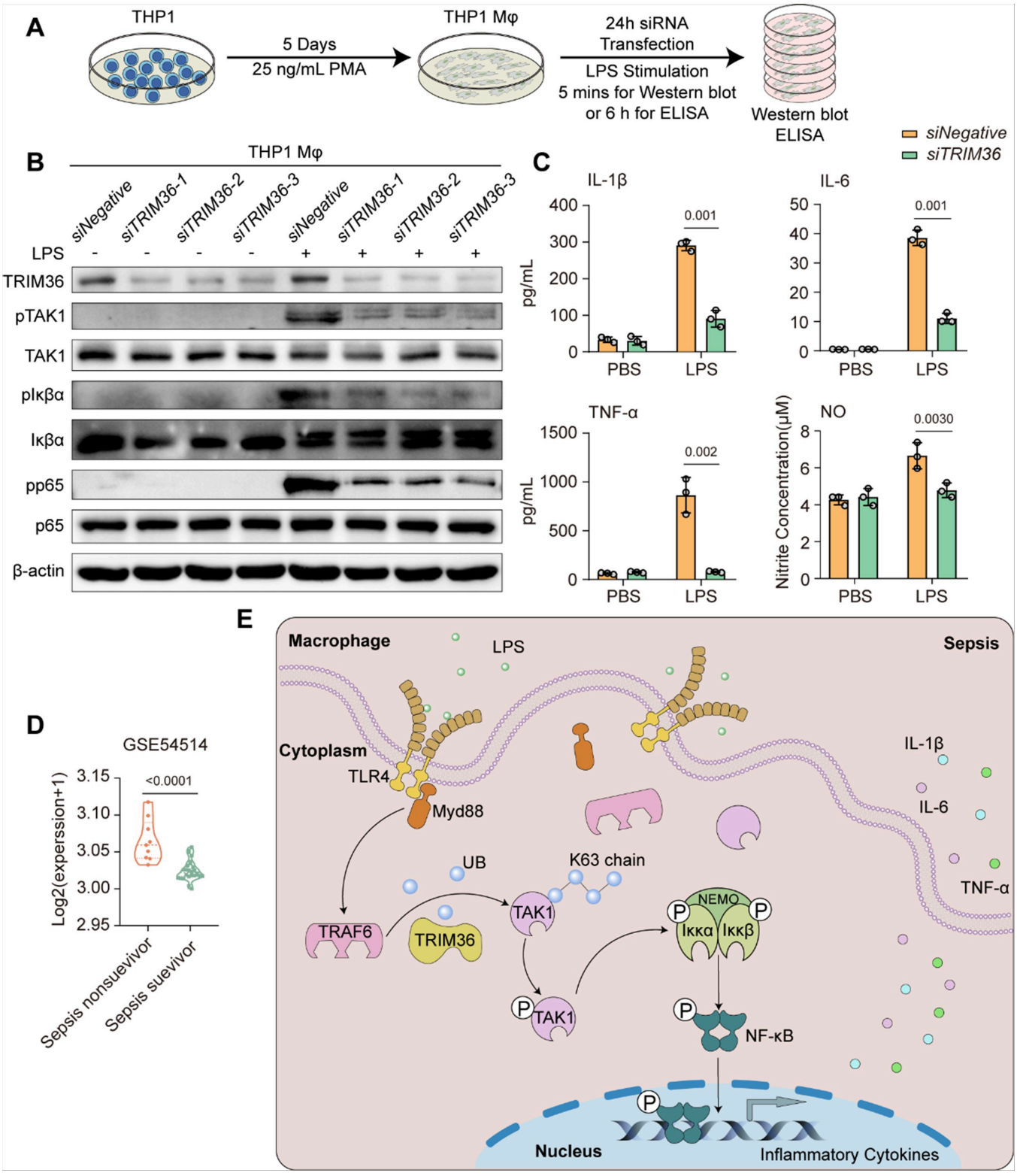


Figure 7

TRIM36 potentiates TLR4 signaling and inflammatory responses in human THP-1 Mφ. (A) Schematic of the experimental workflow. THP-1 monocytes were differentiated into macrophages (THP-1 Mφ) with

PMA (25 ng/mL, 5 days), transfected with siRNAs for 24 h, and then stimulated with LPS (100 ng/mL) for the indicated durations. **(B)** Immunoblot analysis of phosphorylated TAK1, IκBα, and p65 in THP-1 Mφ transfected with control siRNA or siRNAs against TRIM36 (siTRIM36-1, -2, -3), followed by LPS (100 ng/mL, 5 min) stimulation. **(C)** ELISA of IL-1β, IL-6, TNF-α, and NO levels in the culture supernatants of THP-1 Mφ from **(A)**after LPS stimulation (100 ng/mL, 6 h) (n = 3). **(D)**Violin plot showing elevated TRIM36 transcript levels in non-survivors compared to survivors of sepsis, based on analysis of a GEO dataset. Data are presented as mean ± SD. Statistical significance was determined by two-way ANOVA with Sidak's post-hoc test **(C)** and by the *Mann-Whitney U* test (D). **(E)** Working model: TRIM36 acts as a critical signaling amplifier in the TLR4 pathway by binding TAK1 and mediating its K63-linked ubiquitination, which is essential for robust TAK1 and NF-κB activation. This TRIM36-dependent hyper-inflammatory response contributes to pathological inflammation and worsened outcomes in sepsis.

Supplementary Files

This is a list of supplementary files associated with this preprint. Click to download.

- 20260421Supplementarymaterials.docx